Y. Sun[1], Y. Lu[1], L. Chen[2], T. Gao[1], R. D'Souza[1], J.Q. Feng[1], and C. Qin[1]*

[1]Department of Biomedical Sciences, Texas A&M Health Science Center Baylor College of Dentistry, 3302 Gaston Ave., Dallas, TX 75246, USA; and [2]Department of Endodontics, School of Stomatology, Harbin Medical University, Harbin, Heilongjiang 150001, China; *corresponding author, cqin@bcd.tamhsc.edu

# DMP1 Processing is Essential to Dentin and Jaw Formation

## ABSTRACT

Dentin matrix protein 1 (DMP1), an acidic protein that is essential to the mineralization of bone and dentin, exists as proteolytically processed fragments in the mineralized tissues. In this study, we characterized the tooth and jaw phenotypes in transgenic mice containing no wild-type DMP1, but expressing a mutant DMP1 in which Asp[213], a residue at one cleavage site, was replaced by Ala[213] (named "*Dmp1*-KO/*D213A-Tg*" mice). The teeth and mandible of *Dmp1*-KO/*D213A-Tg* mice were compared with those of wild-type, *Dmp1*-knockout (*Dmp1*-KO), and *Dmp1*-KO mice expressing the normal *Dmp1* transgene. The results showed that D213A-DMP1 was not cleaved in dentin, and the expression of D213A-DMP1 failed to rescue the defects in the dentin, cementum, and alveolar bones in the *Dmp1*-KO mice. These findings indicate that the proteolytic processing of DMP1 is essential to the formation and mineralization of dentin, cementum, and jaw bones.

**KEY WORDS:** dentinogenesis, dentin matrix protein 1, proteolytic processing, alveolar bone, cementum.

## INTRODUCTION

Several studies have demonstrated the crucial role of dentin matrix protein 1 (DMP1) in the formation of mineralized tissues (Ye *et al*., 2004, 2005; Feng *et al*., 2006). However, the precise mechanisms by which DMP1 participates in biomineralization are still unclear. Fundamental information about how DMP1 functions in mineralized tissues is necessary for a better understanding of the mechanisms controlling the process of biomineralization.

In the extracellular matrix (ECM) of dentin and bone, DMP1 mainly occurs as the proteolytically processed fragments originating from the $NH_2$-terminal and COOH-terminal regions of the DMP1 amino acid sequence (Qin *et al*., 2003). The $NH_2$-terminal fragment of DMP1 (designated as "DMP1-N") exists in two forms: the 37-kDa fragment (Qin *et al*., 2003) and the proteoglycan form referred to as "DMP1-PG" (Qin *et al*., 2006), while the COOH-terminal fragment (designated as "DMP1-C") is present as the 57-kDa fragment (Qin *et al*., 2003). Recently, the full-length form of DMP1 has been detected in the ECM of bone and dentin at a remarkably lower level than in its processed fragments (Huang *et al*., 2008).

*In vitro* studies showed that DMP1-C promotes the nucleation and growth of hydroxyapatite crystals (Tartaix *et al*., 2004; Gajjeraman *et al*., 2007), while DMP1-PG, the proteoglycan form of the $NH_2$-terminal fragment of DMP1, inhibited mineral formation in a dose-dependent manner (Gericke *et al*., 2010). In addition, the distribution of DMP1-N in the tooth is different from that of DMP1-C: The former is mainly located in the predentin, while the latter is primarily present in the mineralized dentin (Maciejewska *et al*., 2009a). These findings support the speculation that the proteolytic processing of DMP1 is an activation step that releases functional fragments from the inactive full-length precursor.

Protein chemistry work has shown that rat DMP1 is processed into the $NH_2$-terminal and COOH-terminal fragments at 4 peptide bonds (Qin *et al*., 2003): Phe[189]-Asp[190], Ser[196]-Asp[197], Ser[233]-Asp[234], and Gln[237]-Asp[238]. (Note that amino acids are numbered from the $NH_2$-terminus of the signal peptide, not from the $NH_2$-terminus of the secreted protein.) The amino acid sequence alignment shows that residues Ser[196] and Asp[197] and their flanking regions in the rat DMP1 are highly conserved across a broad range of species, suggesting that the proteolytic cleavage at this site may be related to an important biological function (Qin *et al*., 2004). *In vitro* studies have shown that bone morphogenetic protein-1 (BMP-1)/Tolloid-like proteinases cleave rat DMP1 at the Ser[196]-Asp[197] peptide bond (Steiglitz *et al*., 2004). Furthermore, the replacement of Asp[213] by Ala[213] in mouse DMP1, which corresponds to Asp[197] in rat DMP1, blocked the cleavage of mouse DMP1 (D213A-DMP1) in transfected cells (Peng *et al*., 2009). More recently, we generated transgenic mice

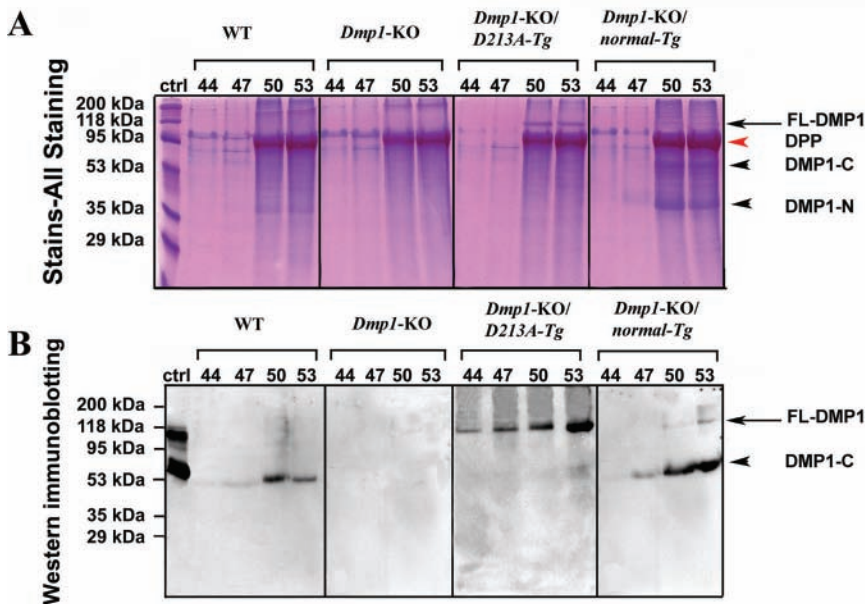**Figure 1.** Detection of DMP1 in NCP extracts of dentin from six-week-old WT, *Dmp1*-KO, *Dmp1*-KO/*D213A-Tg*, and *Dmp1*-KO/*normal-Tg* mice. **(A)** We performed Stains-All staining to visualize the DMP1-related components and other NCPs. NCPs were extracted from the dentin of six-week-old WT, *Dmp1*-KO, *Dmp1*-KO/*D213A-Tg*, and *Dmp1*-KO/*normal-Tg* mice. The numbers on top of each figure represent the anion-exchange chromatographic fractions. A 60-µL quantity of sample from every third fraction between 44 and 53 was loaded onto SDS-PAGE. DMP1-N and DMP1-C fragments (black arrowheads) were observed in the dentin extracts from WT and *Dmp1*-KO/*normal-Tg* mice. Full-length DMP1 (between the 95 kDa and 118 kDa molecular-weight markers; indicated by black arrows) was clearly detected in the dentin extract from the *Dmp1*-KO/*D213A-Tg* mice; our previous work (Huang *et al.*, 2008) showed that full-length DMP1 migrates at this position. The identification of this protein band as DMP1 was further confirmed by Western immunoblotting (see below). A weak protein band representing full-length DMP1 was also seen in the dentin extract from the *Dmp1*-KO/*normal-Tg* mice. The broad protein band migrating just below the 95-kDa molecular marker in fractions 50 and 53 represents dentin phosphoprotein (DPP, red arrowhead), which co-eluted with DMP1 in these fractions. DPP could be considered an internal control, showing that the total amount of proteins loaded onto each SDS-PAGE well was similar among the different groups. **(B)** Western immunoblotting was performed with the anti-DMP1-C-857 antibody. The volume and identities of the samples were the same as in Stains-All staining (Fig. 1A). Ctrl: 2 µg of DMP1 (including full-length and fragments) isolated from rat long bone was used as a positive control (ctrl). The protein bands migrating between the 95-kDa and 118-kDa molecular markers (black arrow) represent the full-length form of DMP1. The arrowheads indicate DMP1-C (~57 kDa). Only DMP1-C was observed in the WT mice. No protein bands were detected in the *Dmp1*-KO mice. Only the full-length form of DMP1 was detected in the *Dmp1*-KO/*D213A-Tg* mice when this volume (60 µL) of sample was loaded. Both the full-length and fragment forms of DMP1 were detected in the *Dmp1*-KO/*normal-Tg* mice. The above findings indicate that normal DMP1 was cleaved into fragments, whereas D213A-DMP1 was not.

containing no wild-type DMP1, but expressing a mutant DMP1, in which Asp[213] was replaced by Ala[213] (named *Dmp1*-KO/*D213A-Tg* mice) (Sun *et al.*, 2010a). The substitution of Asp[213] by Ala[213] in the mouse DMP1 blocked the cleavage of DMP1 in bone, and the expression of the mutant DMP1 failed to rescue the defects in the long bone of *Dmp1* knockout (*Dmp1*-KO) mice. In this study, we characterized the dentin, cementum, alveolar bone, and mandibular phenotypes in *Dmp1*-KO/*D213A-Tg* mice.

## MATERIALS & METHODS

### Generation of *Dmp1*-KO/*D213A-Tg* Mice

A pBC-KS construct containing a 3.6-kB rat *Col 1a1* promoter in the upstream of the mouse DMP1 cDNA was used to generate the targeting transgene (Lu *et al.*, 2007; Sun *et al.*, 2010a). Site-directed mutagenesis was performed on this construct to generate the transgene encoding D213A-DMP1 (designated as the "*Dmp1-D213A*" transgene). Founders that expressed the *Dmp1-D213A* transgene in a C57BL/6J background were crossbred to the *Dmp1* knockout (*Dmp1*-KO) mice (Feng *et al.*, 2003; Ye *et al.*, 2004, 2005) to generate mice that express the *D213A-Dmp1* transgene but lack endogenous *Dmp1* (designated *Dmp1*-KO/*D213A-Tg* mice). PCR genotyping and real-time reverse-transcription PCR were performed with RNA isolated from the bone of *Dmp1*-KO/*D213A-Tg* mice as a template to assess the expression level of the *D213A-Dmp1* transgene in these mice (Sun *et al.*, 2010a).

In this study, we characterized the tooth and mandible phenotypes from 3 lines of *Dmp1*-KO/*D213A-Tg* mice expressing different levels of the *D213A-Dmp1* transgene. The line with the highest level of transgene expression was used for protein chemistry, radiological, and morphological analyses. The dentin, cementum, and mandibular phenotypes of *Dmp1*-KO/*D213A-Tg* mice were compared with those of (1) wild-type (WT), (2) *Dmp1*-KO, and (3) *Dmp1*-KO mice expressing the normal *Dmp1* transgene (*Dmp1*-KO/*normal-Tg*) under the type I collagen promoter. Details regarding the generation and characteristics of the *Dmp1*-KO/*normal-Tg* mice have been reported (Lu *et al.*, 2007). All of the animal protocols used in this study were approved by the Animal Welfare Committee of Texas A&M Health Science Center Baylor College of Dentistry.

### Extraction and Separation of Non-collagenous Proteins (NCPs) from Dentin

NCPs were extracted from the dentin of incisors of 5 six-week-old WT, *Dmp1*-KO, *Dmp1*-KO/*D213A-Tg*, and *Dmp1*-KO/ *normal-Tg* mice by 4 M guanidinium chloride/0.5 M ethylenediaminetetraacetic acid, as previously described (Sun *et al.*, 2010b). The

extracted NCPs were separated by Q-Sepharose (Amersham Biosciences, Uppsala, Sweden) chromatography as previously described (Sun *et al.*, 2010b). The Q-Sepharose column separated NCPs into 120 0.5-mL fractions.

## Detection of Full-length DMP1 and its Fragments

The chromatographic fractions were analyzed by sodium dodecyl sulfate-polyacrylamide gel electrophoresis (SDS-PAGE) with Stains-All staining and Western immunoblotting. For the Western immunoblotting, the affinity-purified anti-DMP1-C-857 antibody (Maciejewska *et al.*, 2009b) was used at a concentration of 0.2 µg IgG/mL. The secondary antibody was alkaline-phosphate-conjugated anti-rabbit IgG (Sigma-Aldrich, St. Louis, MO, USA) at a dilution of 1:5000. The blots were incubated in CDP-star (Ambion, Austin, TX, USA) for 5 min and exposed to x-ray films.

## Micro-CT Analysis

We used a Scanco Medical micro-CT35 (Scanco, Wayne, PA, USA) to analyze the structure of the mandibles from six-week-old WT, *Dmp1*-KO, *Dmp1*-KO/*normal-Tg*, and *Dmp1*-KO/*D213A-Tg* mice. The mandibles of one-year-old WT and *Dmp1*-KO/*D213A-Tg* mice were also evaluated to show the changes associated with aging. High-resolution scans (3.5 µm/slice) and three-dimensional reconstructions were carried out for an overall assessment of the morphologic characteristics of the mouse mandibles.

## Tissue Preparation and Histology Analysis

Under anesthesia, the aforementioned six-week-old and one-year-old mice were perfused with 4% paraformaldehyde in phosphate-buffered solution. The mandibles were dissected and decalcified in 8% EDTA. The tissues were processed for paraffin embedding, and 5-µm serial sections were prepared. We used hematoxylin and eosin (H&E) staining to evaluate the phenotypes in the dentin, cementum, alveolar bone, and the body of the mouse mandible.

## Double Fluorochrome Labeling

We carried out calcein-green/Alizarin red fluorochrome double labeling (Feng *et al.*, 2006) to examine the mineral deposition rate in the dentin of the WT, *Dmp1*-KO, and *Dmp1*-KO/
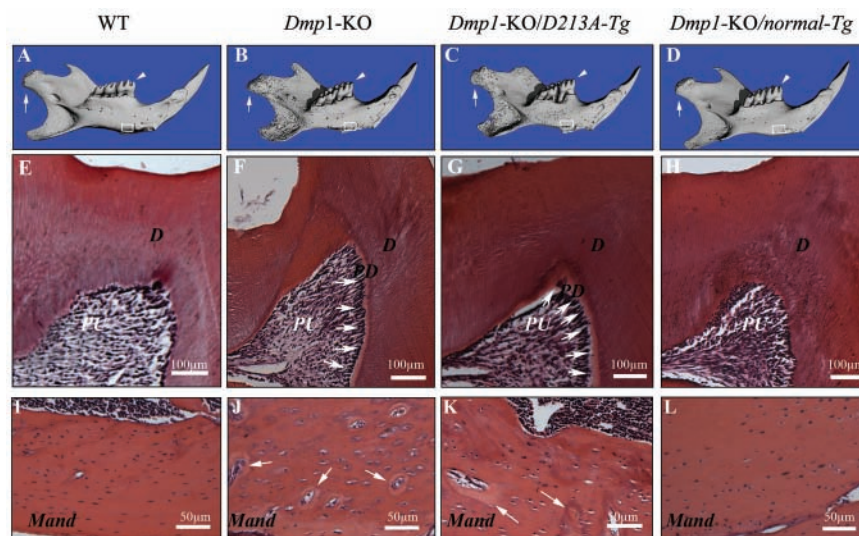


**Figure 2.** Micro-CT images and H&E staining of the teeth and mandibles of the six-week-old mice. PD = predentin; D = dentin; PU = pulp; Mand = mandibular body. **(A-D)** Micro-CT images of the mandibles: WT, *Dmp1*-KO, *Dmp1*-KO/*D213A-Tg*, and *Dmp1*-KO/*normal-Tg* mice. The condyles were indicated by white arrows, the first molars analyzed by H&E staining were indicated by white arrowheads (E-H), and the mandibular areas analyzed by H&E staining were boxed (I-L). The three-dimensional micro-CT images showed that the mandibles of the *Dmp1*-KO (B) or *Dmp1*-KO/*D213A-Tg* mice (C) were shorter than those of the WT (A) or *Dmp1*-KO/*normal-Tg* mice (D). Compared with the WT and *Dmp1*-KO/*normal-Tg* mice (A,D), the surfaces of the mandibles in the *Dmp1*-KO or *Dmp1*-KO/*D213A-Tg* mice appeared more porous (B,C). **(E-H)** H&E staining of the mesio-cusp region of the first molars of six-week-old mice: WT, *Dmp1*-KO, *Dmp1*-KO/*D213A-Tg*, and *Dmp1*-KO/*normal-Tg* mice. Note that the predentin in the first molars of both *Dmp1*-KO and *Dmp1*-KO/*D213A-Tg mice* (F,G; white arrows) was wider than in the WT (E) or *Dmp1*-KO/*normal-Tg* (H) mice. **(I-L)** H&E staining for the mandibular bodies of six-week-old mice: WT, *Dmp1*-KO, *Dmp1*-KO/*D213A-Tg*, and *Dmp1*-KO/*normal-Tg* mice. Note that the mandibular bodies of both the *Dmp1*-KO and *Dmp1*-KO/*D213A-Tg* mice (J,K) contained more osteoid (areas indicated by white arrows) and enlarged osteocyte lacunae compared with both the WT and *Dmp1*-KO/*normal-Tg* mouse (I,L).

*D213A-Tg* mice. Briefly, 5 mg/kg calcein-green (Sigma-Aldrich) was injected into the abdominal cavities of five-week-old mice, and 20 mg/kg Alizarin red (Sigma-Aldrich) was injected 1 wk later. The mice were sacrificed 48 hrs after the injection of Alizarin red, and the mandibles from these mice were dehydrated and embedded in methylmethacrylate. Sections (10 µm) were cut and viewed under epifluorescent illumination with a Nikon E800 microscope interfaced with Osteomeasure histomorphometry software (Feng *et al.*, 2006). We measured the average distance between the 2 fluorescence labels to compare the difference in the mineral deposition rates of the incisor dentin (cross-section of incisors under the mesial root of the first molar) among the WT, *Dmp1*-KO, and *Dmp1*-KO/*D213A-Tg* mice (4 measurements *per* tooth, n = 6 for each group). Data analyses were performed by a one-way ANOVA for multiple group comparisons and the Bonferroni method for two-group comparisons. The quantified results are represented as the mean ± standard error (SEM). $P < 0.05$ was considered statistically significant.
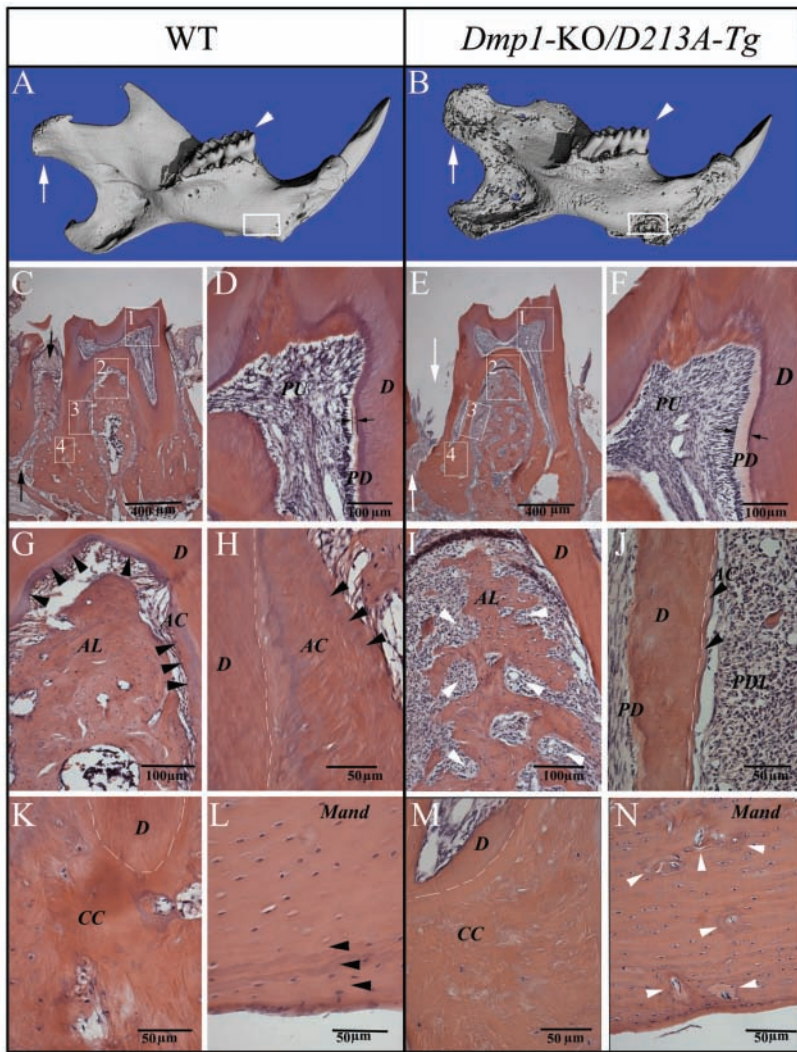
**Figure 3.** Micro-CT images and H&E staining for the teeth and mandibles of one-year-old WT and *Dmp1*-KO/*D213A-Tg* mice. PD = predentin; D = dentin; PU = pulp; AC = acellular cementum; CC = cellular cementum; AL = alveolar bone; Mand = mandibular body. **(A,B)** Micro-CT images of the mandibles of one-year-old WT and *Dmp1*-KO/*D213A-Tg* mice: At the age of 1 yr, the phenotypic changes in the *Dmp1*-KO/*D213A-Tg* mouse mandible (B) became more remarkable than in the WT control (A) and more profound compared with the younger mice. The condyles were indicated by white arrows, the first molars analyzed by H&E staining were indicated by white arrowheads (C,E), and the mandibular areas analyzed by H&E staining were boxed (L,N). **(C,E)** H&E staining of the first molars of a one-year-old WT mouse and a one-year-old *Dmp1*-KO/*D213A-Tg* mouse. Note: Compared with the WT control (black arrows in C), the alveolar bone loss (white arrows in E) was obvious. **(D,F)** Higher magnification of the #1 boxed area (predentin and dentin) areas in C and E. Note: The predentin in the *Dmp1*-KO/*D213A-Tg* mouse molar (F) was wider than in the WT (D). **(G,I)** Higher magnification of the #2 boxed areas in C and E showing an enlarged view of the bifurcation region of the WT mouse and the *Dmp1*-KO/*D213A-Tg* mouse. Note the insufficient amounts of alveolar bone in the *Dmp1*-KO/*D213A-Tg* mice (white arrowheads in I). **(H,J)** Root region of the first molar (#3 boxed areas) from the WT mouse and the *Dmp1*-KO/*D213A-Tg* mouse. Note the presence of acellular cementum in the WT mouse and the lack of acellular cementum in the *Dmp1*-KO/*D213A-Tg* mouse (J). White dotted lines indicate the border between the root dentin and cementum. **(K,M)** H&E staining for the apical region of the first molar (#4 boxed areas) from the WT mouse and the *Dmp1*-KO/*D213A-Tg* mouse. **(L,N)** H&E staining for the mandibular body of the WT mouse and *Dmp1*-KO/*D213A-Tg* mouse. Note the presence of a normal lamellar bone structure in the surface areas of the WT mandibular body (black arrowheads in L); compared with the WT mouse, the mandibular body of the *Dmp1*-KO/*D213A-Tg* mouse had more osteoid (gray areas indicated by white arrowheads in N), enlarged osteocyte lacunae, and loss of lamellar bone structure in the surface area.

## RESULTS

### Detection of DMP1 in NCP Extracts from Dentin Matrix

When a 60-μL quantity of sample from fractions 44 to 53 was loaded to SDS-PAGE, Stains-All staining (Fig. 1A) revealed the presence of full-length DMP1 in the *Dmp1*-KO/*D213A-Tg* and *Dmp1*-KO/*normal-Tg* mice. Western immunoblotting (Fig. 1B) with the anti-DMP1-C-857 antibody revealed the presence of a DMP1-C (57 kDa) fragment in the dentin extracts from the WT mice and *Dmp1*-KO/*normal-Tg* mice. In the *Dmp1*-KO/*D213A-Tg* mice, significant amounts of full-length DMP1 (~105 kDa) were detected, while its fragments were barely detectable. When a larger volume of the urea-containing sample (*e.g.*, 300 μL of sample concentrated in a small volume by dialysis and freeze-drying) was loaded on SDS-PAGE, a very weak protein band matching the migration rate of DMP1-C was observed (data not shown). No protein bands were detected by this antibody in the sample from the *Dmp1*-KO mice. These findings indicated that the proteolytic processing of DMP1 was effectively blocked in the dentin of the *Dmp1*-KO/*D213A-Tg* mice.

### Micro-CT Three-dimensional Analyses

Micro-CT analyses showed that the six-week-old mandibular phenotypes of the *Dmp1*-KO/*normal-Tg* mice (Fig. 2D) were similar to those of the WT mice (Fig. 2A), while those of the *Dmp1*-KO/*D213A-Tg* mouse (Fig. 2C) resembled those of the *Dmp1*-KO mice (Fig. 2B). As in the *Dmp1*-KO mice, the outer surface of the mandible in the *Dmp1*-KO/*D213A-Tg* mice appeared rough and porous. The condyle in the *Dmp1*-KO/*D213A-Tg* mice was poorly developed compared with that in WT or *Dmp1*-KO/*normal-Tg* mice. The differences in the micro-CT imaging between the *Dmp1*-KO/*D213A-Tg* and the WT mice became more remarkable with advancing age (Figs. 3A, 3B). The results from the micro-CT analyses indicated that the phenotypic defects in the mandible of the *Dmp1*-KO mice were rescued by the expression of normal DMP1, but not by the mutant D213A-DMP1.

## Histological Changes in *Dmp1*-KO/*D213A-Tg* Mice

The predentin in the molars of six-week-old *Dmp1*-KO/*D213A-Tg* mice (Fig. 2G) was much wider than that of WT or *Dmp1*-KO/*normal-Tg* mice (Figs. 2E, 2H) and was similar to that seen in the *Dmp1*-KO mouse (Fig. 2F). Compared with the WT and *Dmp1*-KO/*normal-Tg* mouse (Figs. 2I, 2L), the mandibular bodies of the *Dmp1*-KO and *Dmp1*-KO/*D213A-Tg* (Figs. 2J, 2K) mice contained more osteoid (areas indicated by white arrows) and enlarged osteocyte lacunae. At the one-year-old age, the mineralization defects in the dentin *of Dmp1*-KO/*D213A-Tg* mice became more obvious (see the predentin thicknesses in Figs. 3D and 3F). The phenotypic changes in the alveolar bone and acellular/cellular cementum of one-year-old *Dmp1*-KO/*D213A-Tg* mice (Figs. 3E, 3I, 3J, and 3M) were also distinct: The *Dmp1*-KO/*D213A-Tg* mice had considerably less alveolar bone and acellular/cellular cementum compared with the WT mice (Figs. 3C, 3G, 3H, and 3K, indicated by black arrowheads). Additionally, the mandibular body in the *Dmp1*-KO/*D213A-Tg* mice (Fig. 3N) contained more osteoid than that of the WT mice (Fig. 3L).

## Double Fluorochrome Labeling

We used the average mineral deposition rate (measurement of average distance between the two fluorescent-labeled zones) to calculate the rate of dentin mineralization (Fig. 4). Compared with the WT mice, the mineral deposition rate of the *Dmp1*-KO/*D213A-Tg* mice was significantly slower. The rate of dentin formation in the *Dmp1*-KO/*D213A-Tg* mice was similar to that in the *Dmp1*-KO mice.

## DISCUSSION

Under physiological conditions, DMP1 is mainly present as DMP1-N (including a 37-kDa fragment and DMP1-PG) and DMP1-C fragments in the extracellular matrices of dentin and bone (Qin *et al.*, 2003, 2006), while the full-length form of DMP1 is found only in very minor amounts (Huang *et al.*, 2008). The results from this study showed that the dentin of the *Dmp1*-KO/*D213A-Tg* mice contained significant amounts of full-length DMP1 and only trace amounts of DMP1 fragments. Such trace amounts may be attributed to the presence of a redundant peptide bond serving as a cryptic cleavage site. It is obvious that the trace amounts of DMP1 fragments were far from sufficient to maintain the functions of DMP1, since the dental and jaw phenotypes in the *Dmp1*-KO/*D213A-Tg* mice were similar to those of the *Dmp1*-KO mice.
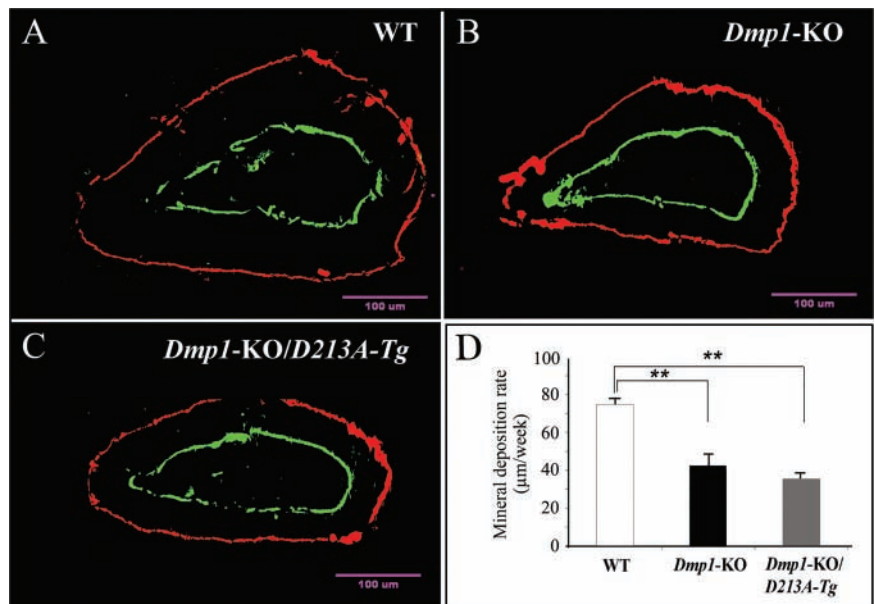


**Figure 4.** Double fluorochrome labeling. The specimens were from the cross-section of incisors under the mesial root of the first molars of six-week-old mice: WT (**A**), *Dmp1*-KO (**B**), and *Dmp1*-KO/*D213A-Tg* (**C**). The labeling was viewed at higher magnification under a fluorescent microscope. We used the distance between these 2 fluorescence-labeled zones to calculate the dentin mineral deposition rate of the incisors. (**D**) The mineral deposition rate of dentin in the WT mice was significantly higher than that in the *Dmp1*-KO or *Dmp1*-KO/*D213A-Tg* mice. For each group, 4 measurements *per* tooth, n = 6 for each group. Data are expressed as mean ± SEM. **p < 0.01.

One of the major histopathological findings from the *Dmp1*-KO mice is the widening of the predentin (Ye *et al.*, 2004), resulting from a failure in the conversion of predentin to dentin at an appropriate rate. The *Dmp1*-KO/*D213A-Tg* mice, which express DMP1 that cannot be properly processed, also showed a widening of the predentin, similar to that seen in the *Dmp1*-KO mice. These findings indicate that the processed fragments of DMP1—not its full-length form—are needed for the conversion of predentin to dentin.

DMP1 is expressed not only in dentin and bone but also in cementum at a significant level (Baba *et al.*, 2004). A recent study showed that the deletion of DMP1 leads to an increased susceptibility to periodontal diseases in mice, suggesting that DMP1 is essential for the formation and maintenance of a healthy periodontium (Ye *et al.*, 2008). The defects in the alveolar bone and cementum of the *Dmp1*-KO/*D213A-Tg* mice resembled those seen in the *Dmp1*-KO mice (*e.g.*, lack of sufficient amounts of alveolar bone and cementum), indicating that proper processing of DMP1 is necessary for the integrity of the periodontal tissues. The insufficient amounts of alveolar bone and cementum observed in the *Dmp1*-KO mice and *Dmp1*-KO/D213A-Tg mice may be due to two factors: (1) developmental defects, leading to the decrease in the deposition of alveolar bone and cementum; and (2) gradual loss, resulting from the absorption of the poor-quality bone and cementum in these mutant mice.

Previous studies showed that the expression of the normal *Dmp1* transgene or DMP1-C terminal fragments driven by a 3.6-kB rat *Col 1a1* promoter (the same as the one used in this

study) fully rescued the skeletal and dental phenotypes of *Dmp1*-KO mice (Lu *et al.*, 2007, 2009, 2011). Our recent study showed that the expression of D213A-DMP1, which could not be processed into fragments, failed to rescue the defects in the long bone of *Dmp1*-KO mice (Sun *et al.*, 2010a). This study demonstrated that the expression of D213A-DMP1 could not correct the abnormal structures of dentin, cementum, alveolar bone, and the mandible in the *Dmp1*-KO mice. These findings lend further support to our hypothesis that the proteolytic processing of DMP1 is an essential activation step for the proper functioning of this protein in biomineralization.

In summary, the observation that the failure of DMP1 to cleave into fragments leads to the inactivation of this protein strongly supports the hypothesis that the proteolytic processing of DMP1 is essential for the function of this protein during biomineralization. The findings from this study provide the basic foundation for future investigations regarding the physical interactions between the active fragments of DMP1 and other components in the ECM of mineralized tissues.

## ACKNOWLEDGMENTS

## REFERENCES

Baba O, Qin C, Brunn JC, Wygant JN, Mcintyre BW, Butler WT (2004). Colocalization of dentin matrix protein 1 and dentin sialoprotein at late stages of rat molar development. *Matrix Biol* 23:371-379.

Feng JQ, Huang H, Lu Y, Ye L, Xie Y, Tsutsui TW*, et al*. (2003). The dentin matrix protein 1 (Dmp1) is specifically expressed in mineralized, but not soft, tissues during development. *J Dent Res* 82:776-780.

Feng JQ, Ward LM, Liu S, Lu Y, Xie Y, Yuan B*, et al*. (2006). Loss of DMP1 causes rickets and osteomalacia and identifies a role for osteocytes in mineral metabolism. *Nat Genet* 38:1310-1315.

Gajjeraman S, Narayanan K, Hao J, Qin C, George A (2007). Matrix macromolecules in hard tissues control the nucleation and hierarchical assembly of hydroxyapatite. *J Biol Chem* 282:1193-1204.

Gericke A, Qin C, Sun Y, Redfern R, Redfern D, Fujimoto Y*, et al*. (2010). Different forms of DMP1 play distinct roles in mineralization. *J Dent Res* 89:355-359.

Huang B, Maciejewska I, Sun Y, Peng T, Qin D, Lu Y*, et al*. (2008). Identification of full-length dentin matrix protein 1 in dentin and bone. *Calcif Tissue Int* 82:401-410.

Lu Y, Ye L, Yu S, Zhang S, Xie Y, McKee MD*, et al*. (2007). Rescue of odontogenesis in Dmp1-deficient mice by targeted re-expression of DMP1 reveals roles for DMP1 in early odontogenesis and dentin apposition *in vivo*. *Dev Biol* 303:191-201.

Lu Y, Qin C, Xie Y, Bonewald LF, Feng JQ (2009). Studies of the DMP1 57-kDa functional domain both *in vivo* and *in vitro*. *Cells Tissues Organs* 189:175-185.

Lu Y, Yuan B, Qin C, Cao Z, Xie Y, Dallas S*, et al*. (2011). The biological function of DMP1 in osteocyte maturation is mediated by its 57 kDa C-terminal fragment. *J Bone Miner Res* [Epub ahead of print, August 29, 2011] (in press).

Maciejewska I, Cowan C, Svoboda K, Butler WT, D'Souza R, Qin C (2009a). The NH2-terminal and COOH-terminal fragments of dentin matrix protein 1 (DMP1) localize differently in the compartments of dentin and growth plate of bone. *J Histochem Cytochem* 57:155-166.

Maciejewska I, Qin D, Huang B, Sun Y, Mues G, Svoboda K*, et al*. (2009b). Distinct compartmentalization of dentin matrix protein 1 fragments in mineralized tissues and cells. *Cells Tissues Organs* 189:186-191.

Peng T, Huang B, Sun Y, Lu Y, Bonewald L, Chen S*, et al*. (2009). Blocking of proteolytic processing and deletion of glycosaminoglycan side chain of mouse DMP1 by substituting critical amino acid residues. *Cells Tissues Organs* 189:192-197.

Qin C, Brunn JC, Cook RG, Orkiszewski RS, Malone JP, Veis A*, et al*. (2003). Evidence for the proteolytic processing of dentin matrix protein1. Identification and characterization of processed fragments and cleavage sites. *J Biol Chem* 278:34700-34708.

Qin C, Baba O, Butler WT (2004). Post-translational modifications of SIBLING proteins and their roles in osteogenesis and dentinogenesis. *Crit Rev Oral Biol Med* 15:126-136.

Qin C, Huang B, Wygant JN, McIntyre BW, McDonald CH, Cook RG*, et al*. (2006). A chondroitin sulfate chain attached to the bone dentin matrix protein 1 NH$_2$-terminal fragment. *J Biol Chem* 281:8034-8040.

Steiglitz BM, Ayala M, Narayanan K, George A, Greenspan DS (2004). Bone morphogenetic protein-1/Tolloid-like proteinases process dentin matrix protein-1. *J Biol Chem* 279:980-986.

Sun Y, Prasad M, Gao T, Wang X, Zhu Q, D'Souza R*, et al*. (2010a). Failure to process dentin matrix protein 1 (DMP1) into fragments leads to its loss of function in osteogenesis. *J Biol Chem* 285:31713-31722.

Sun Y, Lu Y, Chen S, Prasad M, Wang X, Zhu Q*, et al*. (2010b). Key proteolytic cleavage site and full-length form of DSPP. *J Dent Res* 89:498-503.

Tartaix PH, Doulaverakis M, George A, Fisher LW, Butler WT, Qin C*, et al*. (2004). *In vitro* effects of dentin matrix protein-1 on hydroxyapatite formation provide insights into *in vivo* functions. *J Biol Chem* 279: 18115-18120.

Ye L, MacDougall M, Zhang S, Xie Y, Zhang J, Li Z*, et al*. (2004). Deletion of dentin matrix protein-1 leads to a partial failure of maturation of predentin into dentin, hypomineralization, and expanded cavities of pulp and root canal during postnatal tooth development. *J Biol Chem* 279:19141-19148.

Ye L, Mishina Y, Chen D, Huang H, Dallas SL, Dallas MR*, et al*. (2005). Dmp1-deficient mice display severe defects in cartilage formation responsible for a chondrodysplasia-like phenotype. *J Biol Chem* 280:6197-6203.

Ye L, Zhang S, Ke H, Bonewald LF, Feng JQ (2008). Periodontal breakdown in the Dmp1 null mouse model of hypophosphatemic rickets. *J Dent Res* 87:624-629.